AGU PUBLICATIONS

Geophysical Research Letters

RESEARCH LETTER
10.1002/2015GL066572

Key Points:
- Interannual blocking variability in the NH is significantly influenced by tropical variability
- Extratropical SST and sea ice is influential especially on decadal timescales
- Half of the observed blocking variability can only be explained by extratropical tropospheric dynamics

Supporting Information:
- Texts S1 and S2 and Figures S1–S7 captions
- Figure S1
- Figure S2
- Figure S3
- Figure S4
- Figure S5
- Figure S6
- Figure S7

Correspondence to:
G. Gollan,
ggollan@geomar.de

Citation:
Gollan, G., R. J. Greatbatch, and T. Jung (2015), Origin of variability in Northern Hemisphere winter blocking on interannual to decadal timescales, *Geophys. Res. Lett.*, *42*, 10,037–10,046, doi:10.1002/2015GL066572.

Received 20 OCT 2015
Accepted 2 NOV 2015
Accepted article online 4 NOV 2015
Published online 21 NOV 2015

Origin of variability in Northern Hemisphere winter blocking on interannual to decadal timescales

Gereon Gollan[1], Richard J. Greatbatch[1,2], and Thomas Jung[3]

[1]GEOMAR Helmholtz Centre for Ocean Research Kiel, Kiel, Germany, [2]Faculty of Mathematics and Natural Sciences, Kiel University, Kiel, Germany, [3]Alfred Wegener Institute, Bremerhaven, Germany

Abstract Variability of midlatitude blocking in the boreal winter Northern Hemisphere is investigated for the period 1960/1961 to 2001/2002 by means of relaxation experiments with the model of the European Centre for Medium-Range Weather Forecasts. It is shown that there is pronounced interannual and decadal variability in blocking, especially over the Eurasian continent, consistent with previous studies. The relaxation experiments show that realistic variability in the tropics can account for a significant part of observed interannual blocking variability but also that about half of the observed variability can only be explained by extratropical tropospheric variability. On the quasi-decadal timescale, extratropical sea surface temperature and sea ice, in addition to tropical variability, play a more important role. The stratosphere, which has been shown to influence interannual variability of the North Atlantic Oscillation in previous studies, has no significant influence on blocking according to our analysis.

1. Introduction

Midlatitude blocking has a strong impact on surface weather and climate, as a blocked situation can cut regions off from the usually prevailing westerlies by distorting the eddy driven jet. Additionally, blocking regimes often persist for longer than expected based on synoptic timescales (e.g., 5–10 days), leading to prolonged cold spells in winter and hot spells in summer [e.g., *Trigo et al.*, 2004; *Sillmann and Croci-Maspoli*, 2009; *Greatbatch et al.*, 2015]. From a dynamical point of view, blocking is associated with upper tropospheric Rossby wave breaking that leads to strong poleward displacement of subtropical air of low potential vorticity [e.g., *Hoskins et al.*, 1985]. Midlatitude blocking frequencies peak over the eastern Atlantic and Europe, while European blocking can act as a precursor for negative regimes of the North Atlantic Oscillation (NAO) [e.g., *Wallace and Gutzler*, 1981; *Woollings et al.*, 2008; *Hurrell and Deser*, 2010]. A good representation of blocking in numerical weather prediction and climate models is therefore important for a wide range of scientific and societal issues; however, most current models have too low blocking frequencies or have difficulties in predicting the timing of blocking [e.g., *Jung et al.*, 2012; *Hamill and Kiladis*, 2014]. *Jung et al.* [2012] found that increasing horizontal resolution from spectral truncation T159 to T511 significantly improves the simulation of blocking frequencies over Europe. In long climate simulations, on the other hand, models today often have a resolution of only T63 [*Flato et al.*, 2013; *Anstey et al.*, 2013].

Decadal variations and possible trends in boreal winter blocking frequencies have been investigated in several earlier studies, some of which suggest that there is an increase in Northern Hemisphere blocking frequency after the year 2000, possibly driven by Arctic sea ice loss [*Francis and Vavrus*, 2012; *Liu et al.*, 2012], others, however, caution that observations do not confirm any hemispheric trend in blocking frequencies [*Barnes et al.*, 2012, 2014]. *Barnes et al.* [2014] show that there has been strong variability in blocking frequencies over the whole modern observational record so that the recent variations do not appear exceptional, and that no external, e.g., anthropogenic, forcing is needed to explain these variations. However, as far as the tropics may be viewed as external to the extratropical atmosphere, there is a possibility for drivers of blocking variability apart from tropospheric internal variability, for example, associated with El Niño Southern Oscillation (ENSO) variability and the associated teleconnections [e.g., *Renwick and Wallace*, 1996; *Hoerling et al.*, 2001; *Woollings et al.*, 2008]. Some authors [e.g., *Renwick and Wallace*, 1996; *Wiedenmann et al.*, 2002; *Barriopedro et al.*, 2006] find that La Niña winters are associated with more frequent and intense blocking in the North Pacific region (weaker blocking during El Niño).

In previous studies concerning possible drivers of variability of major extratropical atmospheric teleconnection patterns using relaxation experiments, we found a strong impact from the tropics and also from the stratosphere [*Greatbatch et al.*, 2012a, 2012b]. Here we investigate the relative impact of the tropical atmosphere, the Northern Hemisphere stratosphere, and extratropical sea surface temperature (SST) and sea ice on the variability of boreal winter (December, January and February: DJF hereafter) blocking frequencies on interannual and quasi-decadal timescales. The plan of this paper is as follows: In section 2 the experimental setup is explained, and the blocking index applied is defined. Results are presented in section 3 followed by a discussion of possible explanations for our results in section 4.

2. Methodology

The idea behind the relaxation experiments used in this study is the evaluation of the impact of perfect forecasts in different regions of the atmosphere on the seasonal predictability in the unrelaxed parts, which is the extratropical troposphere in this case [see, e.g., *Jung et al.*, 2011; *Greatbatch et al.*, 2012a]. Therefore, the Integrated Forecast System, version 36r1, of the European Centre for Medium-Range Weather Forecasts (ECMWF), in spectral horizontal resolution T159 with 60 vertical levels reaching up to 0.1 hPa, is initialized in the beginning of each November between 1960 and 2001 and is then integrated until the end of each following February, only data from the first of December onward being analyzed. Using slightly different initial conditions, 12 realizations are created for each winter and for each experimental setup. Keeping in mind that T159 resolution is not enough to get a fully realistic blocking frequency climatology [*Jung et al.*, 2012], we do not expect the model to simulate the latter perfectly, but comparison between the different experiments gives an estimate about added skill arising from perfect forecasts in the relaxed regions. Thus, anomalies are calculated separately for each model experiment to focus on changes in blocking frequency rather than on the model climatology. The relaxation term is added to the model as follows:

$$-\lambda(x - x_{\mathrm{ref}}). \tag{1}$$

where x represents the model state vector and x_{ref} is the reference field toward which the model is drawn. The parameters relaxed are zonal velocity, u, meridional velocity, v, temperature T, and the logarithm of the surface pressure, ln(ps), using a timescale of 10 h. The reference field the model is drawn to is the time-varying ERA-40 reanalysis [*Uppala et al.*, 2005], and in all our analyses we validate the model against ERA-40 data.

The model experiments are as follows:

1. *CLIM-NO*. Climatological SST and sea ice is specified at the lower boundary and no relaxation is used. The climatology is calculated using SST and sea ice for the period 1979–2002. The only information about the atmospheric state in each year comes from the initial conditions that are thought to be dispersed in the extratropics after not more than 2–3 weeks.
2. *OBS-NO*. Observed SST and sea ice from ERA-40 is specified at the lower boundary and no relaxation is used.
3. *CLIM-TROPICS*. Climatological SST and sea ice (as in CLIM-NO) is specified and relaxation is used between 20°N and 20°S throughout the whole depth of the model atmosphere.
4. *OBS-TROPICS*. Observed SST and sea ice is specified at the lower boundary as in OBS-NO and relaxation is used between 20°N and 20°S as in CLIM-TROPICS. This experiment effectively looks at the additional information gained, compared to CLIM-TROPICS, by specifying the observed SST and sea ice in the extratropics.
5. *CLIM-STRAT-NH*. In this case, climatological SST and sea ice is specified at the lower boundary (as in CLIM-NO) and relaxation towards reanalysis is used in the stratosphere north of 30°N (see *Jung et al.* [2010] for vertical structure of the relaxation strength). Of course, the logarithm of the surface pressure is not relaxed in this experiment.

Barnes et al. [2012] give a review of several blocking detection methods, including one- and two-dimensional indices; many of which are based on the meridional gradient of upper tropospheric potential temperature or of midtropospheric geopotential height. These authors find that, at least when investigating variability in blocking frequency at timescales longer than seasons, geopotential height or zonal wind at 500 hPa, that is usually readily available as model output, can equally be used for the calculation of blocking indices instead of potential temperature. Here we use a modified form of the 1-D index defined in *Masato et al.* [2014],

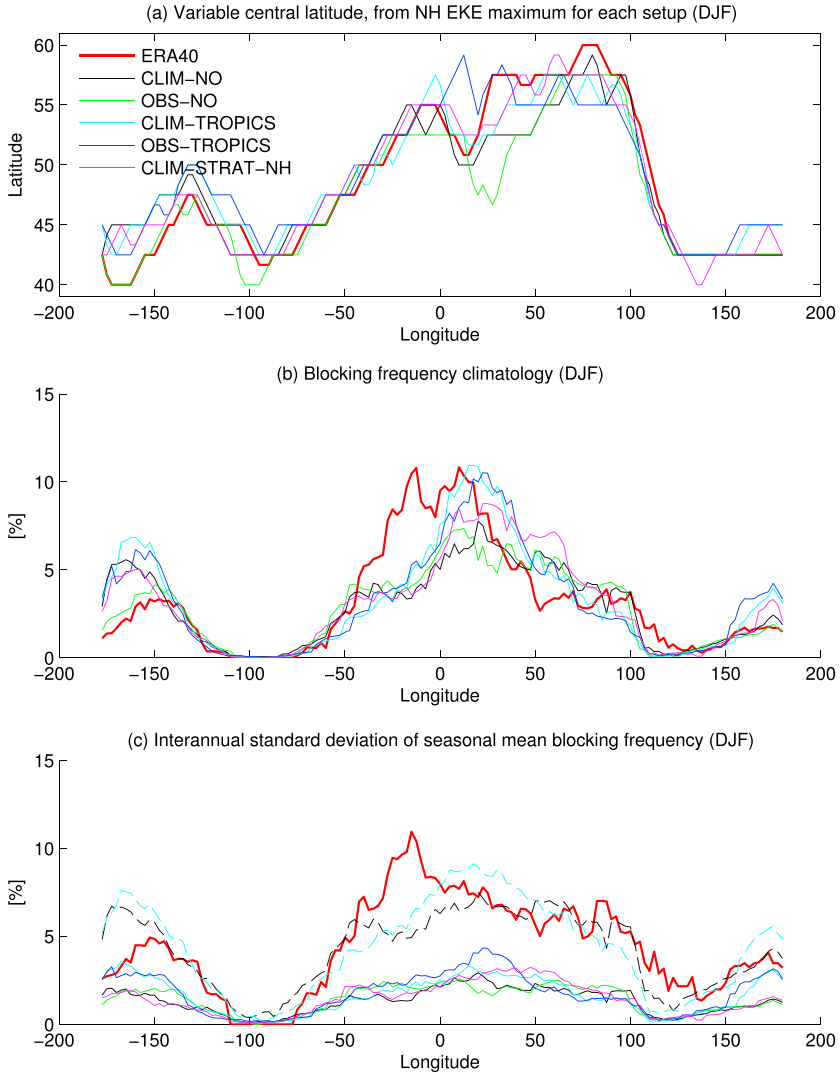

Figure 1. (a) Central blocking latitude, derived from the maximum in transient EKE at 300 hPa for each data set. (b) Blocking frequency climatology for the ERA-40 reanalysis and for each relaxation experiment. (c) Interannual standard deviation of blocking frequency for the ERA-40 reanalysis and for the ensemble mean of each relaxation experiment (the mean for each winter of the BI derived from the single-model realizations). Solid lines indicate the standard deviation for the ensemble means, and dashed lines indicate the standard deviation for all concatenated ensemble members of CLIM-NO and CLIM-TROPICS, respectively. Color coding is the same in each panel, the legend being given only in Figure 1a.

using a variable central blocking latitude (CBL) and 500 hPa geopotential height (Z500) to calculate a daily instantaneous blocking index (BI), defined as the difference between a northern box and a southern box at each longitude (λ), i.e.,

$$BI(\lambda) = \frac{1}{\Delta\phi}\int_{\phi_0}^{\phi_0+\Delta\phi} Z500(\lambda,\phi)\mathrm{d}\phi - \frac{1}{\Delta\phi}\int_{\phi_0-\Delta\phi}^{\phi_0} Z500(\lambda,\phi)\mathrm{d}\phi \quad (2)$$

where $\Delta\phi = 15°$ and ϕ_0 is the CBL. *Barnes et al.* [2012] conclude that it makes sense to use a CBL that follows the climatological position of the storm track that should be computed separately for each data set when comparing between reanalysis data and models or when comparing between different models and model setups. Following *Pelly and Hoskins* [2003] and *Barnes et al.* [2012], the CBL is therefore defined as the latitude of the maximum eddy kinetic energy (EKE) at 300 hPa, which is derived separately for each experiment and for the reanalysis (see Figure 1a). The *u* and *v* anomalies for the calculation of the EKE have been filtered by a

2–6 day band-pass filter to retain synoptic eddies only. The resulting field of EKE has been smoothed spatially by only retaining spectral wave numbers lower than T42, and the resulting CBL is then again smoothed with a 5° longitude running mean. As no trends in the EKE maximum are evident in ERA-40 [*Barnes et al.*, 2012], we use the climatological DJF mean CBL for our calculations.

The CBL therefore represents the position of the climatological midlatitude storm tracks in order to focus on events that actually block the normally eastward propagation of weather systems. Our blocking index does not identify high-latitude blockings poleward of the storm tracks, but those are not the focus of the present study. Model results and reanalysis data have been evaluated on the same grid (2.5° longitude by 2.5° latitude). Slight meridional movement of blocking systems is included by taking the maximum of the instantaneous BI calculated using CBL ±5°. Blocking is then said to occur when the BI is positive for at least five consecutive days and over at least five consecutive longitude grid points (12.5°), the resulting binary blocking index (0: no block, 1: block) being used to calculate seasonal mean blocking frequencies in percent (blocked days per 100 days). Note that the blocking frequencies for the relaxation experiments are derived first using all ensemble members separately, e.g., to create the climatologies shown in Figure 1b and then averaged over all members for each winter to create an ensemble mean.

3. Results

The storm tracks in the different relaxation experiments are in a very similar location as in the reanalysis, i.e., between about 45°N over the east Pacific and about 55°N over Europe (see Figure 1a) except for OBS-NO where the storm tracks are slightly displaced to the south over North America (around 100°W) and over central Europe (around 30°E). The resulting climatologies in boreal winter mean blocking frequency for ERA-40 and the relaxation experiments are shown in Figure 1b. The primary blocking region is centered over Europe and the eastern Atlantic, where blocking frequencies peak around the Greenwich meridian at about 10% in the reanalysis (compare climatologies with those in Figure 7a of *Barnes et al.* [2012]). The climatological blocking peak over the European sector in our experiments is shifted to the east by about 25° and is generally lower compared to the peak in the reanalysis, as in many other models [e.g., *Dunn-Sigouin and Son*, 2013], and only the tropically relaxed experiments, CLIM-TROPICS, and OBS-TROPICS have blocking peaks of a similar magnitude compared to the reanalysis, but still shifted eastward. In the experiment with stratospheric relaxation, blocking frequencies over eastern Europe are also slightly enhanced compared to CLIM-NO and OBS-NO, possibly indicating some effect of downward propagating stratospheric anomalies into the troposphere as, for example, found by *Woollings et al.* [2010]. The secondary climatological blocking peak is over the eastern North Pacific, where the CBL is at about 45°N. Over the eastern North Pacific, blocking frequencies are enhanced in the experiments compared to the reanalysis, again similar to other models [*Dunn-Sigouin and Son*, 2013], and only OBS-NO, the experiment which sees observed SST and sea ice and no relaxation anywhere, has a blocking climatology similar to the reanalysis climatology.

Variability of blocking activity is now analysed by means of seasonal winter mean blocking frequency between 1960/1961 and 2001/2002. The Hovmöller plots of seasonal mean blocking frequency anomalies for ERA-40 (referring to the ERA-40 climatology) and the relaxation experiments are shown in Figure 2. For the experiments, anomalies refer to the departure of the ensemble mean BI from the climatology of each experimental setup (see Figure 1b) and therefore shows the systematic influence from the forcing and initial condition at the beginning of November in each experiment, the latter being shown by CLIM-NO. Note that ensemble mean anomalies are multiplied by a factor of two for the plot in Figure 2, but also that single-model realizations have a comparable level of interannual blocking variability compared to ERA-40 (see Figure 1c). The reduced amplitude can be explained by internal tropospheric variability as expressed by variability between the ensemble members that is smoothed out when averaging over all members.

Looking at blocking variability in the reanalysis, there is a period of anomalously frequent blocking over western Europe and the east Atlantic during the 1960s, which was also accompanied by a period of negative NAO winters [e.g., *Hurrell and Deser*, 2010]. Note, however, that blocking occurrence over Europe and NAO variability is not equivalent, but that strong blocking over Europe can act as a precursor for upstream high-latitude blocking that indeed characterizes a negative NAO regime [*Woollings et al.*, 2008]. The period of high blocking during the 1960s is followed by strongly varying blocking frequencies, with strong blocking every 4 to 10 years over western Europe, becoming less toward the 1990s, consistent with the trend of

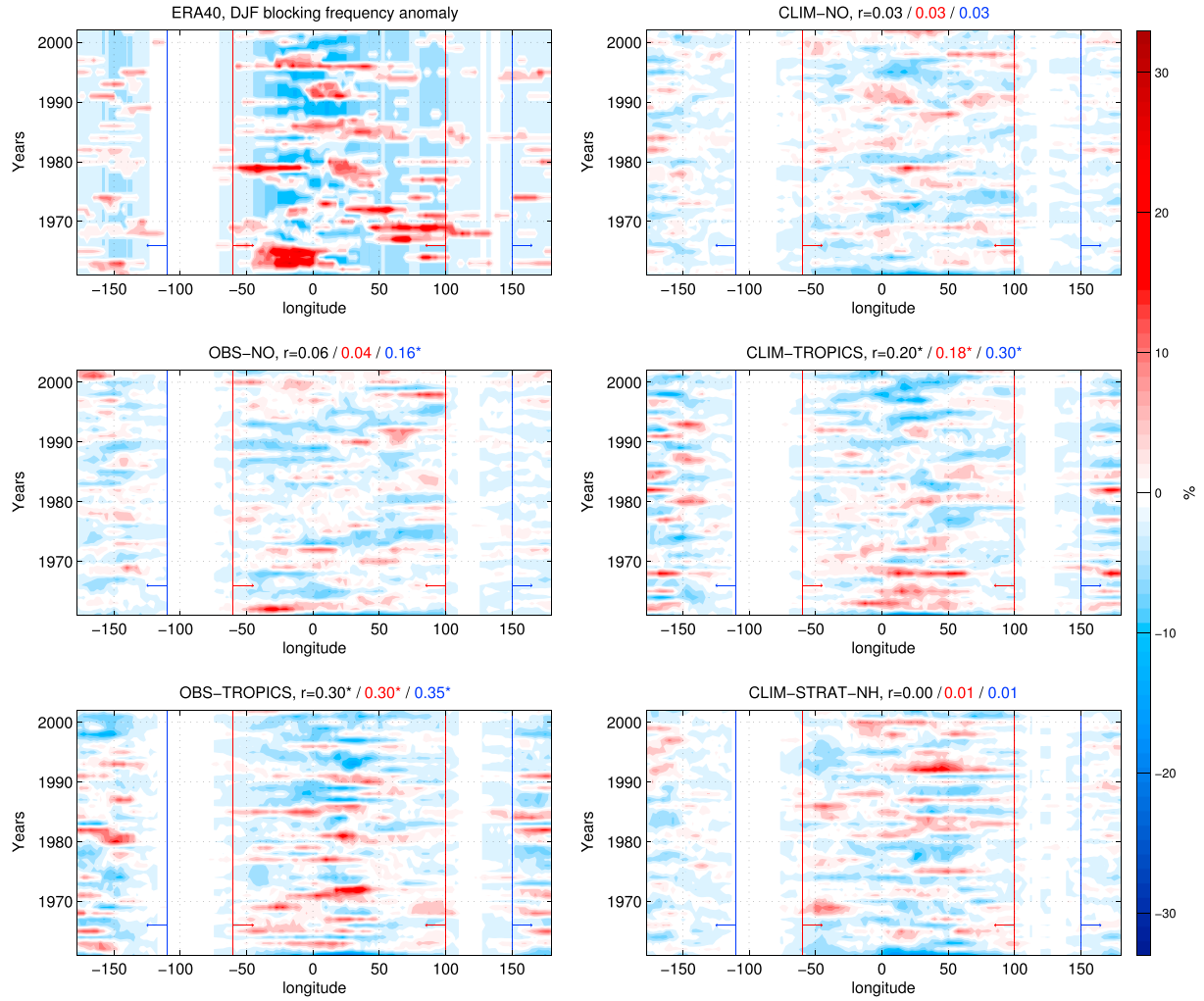

Figure 2. Evolution of anomalous seasonal mean blocking frequency at each longitude from ERA-40 and the relaxation experiments. The anomalies for the relaxation experiments have been multiplied by a factor of 2 to make an easier comparison with those from ERA-40 (see text for discussion). Pattern correlations (in longitude-time space) between the evolution in each experiment and in the reanalysis are given in the title of each panel. Sectors for pattern correlations are all longitudes (black), North Atlantic/Eurasia (red), and Pacific/North America (blue), as indicated by the red/ blue vertical lines in each panel. Correlations marked with asterisks are significant at the 95% level according to a Monte Carlo test (see text for details and supporting information Figure S1).

the NAO toward positive values during that period. Over the Pacific there is a more regular change between winters with high and low blocking frequencies, with no discernable trend occurring in ERA-40 during our analysis period.

To quantify the skill of our relaxation experiments in simulating the observed blocking variability, we show pattern correlation values in the titles of each panel, for the following sectors: All longitudes, Atlantic-Eurasian sector (60°W–100°E) and Pacific-American sector (150°E–110°W). Note that these patterns are in longitude-time space, and that pattern correlation measures similarity between patterns, without respect of the amplitude. The significance of the pattern correlation values is tested by Monte Carlo simulations, shuffling seasonal mean ensemble mean blocking frequencies of all experiments to randomly create 10,000 artificial ensemble means. Shuffling is done in time and between experiments here, while longitude space is not shuffled. The pattern correlations between these artificial ensemble means and the reanalysis are then calculated for all three sectors in the same way as for the original experiments. Then the 95th percentile of the resulting probability distribution of pattern correlations defines the significance threshold (see Figure S1 in the supporting information).

In the relaxation experiments, only the tropically relaxed cases (CLIM-TROPICS and OBS-TROPICS) show a statistically significant skill in simulating the observed variability in both the European and Pacific sectors,

albeit with reduced amplitude. Extratropical SST and sea ice added to realistic tropical variability (OBS-TROPICS) enhance amplitude of ensemble mean blocking anomalies (see Figure 1c) and also the correlation with ERA-40. This is consistent with the hypothesis that variability in Arctic sea ice influences blocking variability over Europe [*Francis and Vavrus*, 2012; *Liu et al.*, 2012], although in our experiments, we cannot distinguish between influence from Arctic sea ice and influence from extratropical SST which could play an important role. In the Pacific sector the experiment without relaxation, but with prescribed SST and sea ice (OBS-NO), shows a small but statistically significant ($r = 0.16$), pattern correlation that is consistent with previous findings that prescribing SST leads to a quite realistic atmospheric variability over the Pacific [e.g., *Trenberth et al.*, 1998; *Greatbatch et al.*, 2012a], even though it is weak compared to the tropically relaxed experiments. The fact that the performance of OBS-NO is weak when concerning the whole Northern Hemisphere or the Atlantic-Eurasian sector, points to the fact that prescribing SST in the tropics can lead to an unrealistic atmospheric response in atmosphere-only models. In particular, convective precipitation tends to occur over anomalously warm SST in such models, whereas in the real world, anomalously warm SST can be driven by enhanced solar radiation under clear sky [e.g., *Wu et al.*, 2006].

To focus on decadal variability of blocking frequency anomalies, supporting information Figure S2 shows a modified version of Figure 2 that is smoothed in time using a 9 year running Hamming mean. Pattern correlations between ensemble means and reanalysis are calculated in the same way as for Figure 2 for the three different sectors and are also tested for significance using the previously described Monte Carlo method. In the reanalysis strong decadal blocking variations can be seen mostly over the European sector. Over western Europe and the eastern Atlantic, high blocking frequencies are found in the mid-1960s and around 1980 and lower blocking frequencies in the early 1970s and between 1985 and 1995, with a hint of increasing blocking frequencies thereafter. These variations are embedded in a trend toward less blocking over the eastern North Atlantic, that is also present as a trend in the 2-D blocking index used by *Woollings et al.* [2008] (see supporting information Figure S4). Over middle Eurasia (between 0° and 100°E), a more complex pattern is found where high blocking frequencies over middle Eurasia (50°E–100°E) until the mid-1970s are gradually displaced to the west until the late 1980s (see supporting information Figure S2). Note that our results for the ERA-40 reanalysis agree generally well with the results by *Barnes et al.* [2014] (who use data from the National Centers for Environmental Prediction/National Center for Atmospheric Research; see their Figure 4) in both the interannual and the decadal variations, as well as for the different sectors.

The decadal evolution over the Atlantic-Eurasian sector is captured only in OBS-TROPICS (where the pattern correlation is significant, $r = 0.38$; see supporting information Figures S1 and S3) although the displacement of blocking from east to west as in the reanalysis is only hinted at in OBS-TROPICS. OBS-NO yields only very low decadal pattern correlations in all sectors (Figure S2). CLIM-TROPICS, while having much in common with OBS-TROPICS, has less skill in capturing the detailed decadal blocking pattern seen in the reanalysis, leading to reduced correlation. Comparing between OBS-NO, CLIM-TROPICS, and OBS-TROPICS on decadal timescales, our results suggest that for low-frequency blocking variability over Europe, extratropical SST and sea ice are influential, but only in combination with realistic tropical atmospheric variability. The stratospheric relaxation experiment (CLIM-STRAT-NH) that showed some skill in simulating interannual and decadal variability in the NAO index [*Greatbatch et al.*, 2012a, 2012b], has no skill in blocking variability on the interannual timescale (Figure 2) or decadal timescale (Figure S2) and only shows some slight similarity over the eastern North Atlantic that is not statistically significant.

Looking at decadal variations over the eastern North Pacific, three periods with relatively high blocking frequencies are found in the reanalysis around the 1970s, the early 1980s, and the early 1990s (see Figure S2). This evolution is captured in both tropically relaxed experiments, with the best performance in CLIM-TROPICS ($r = 0.31$).

4. Discussion

We have shown that the use of a relaxation technique to realistically represent variability in the tropics improves both the climatology and the variability of blocking frequency in the ECMWF model compared to the ERA-40 reanalysis (see Figures 1, 2, and S2). Experiment CLIM-NO, in particular, that distinguishes between each individual winter only through the initial conditions shows no skill compared to the reanalysis in this version of the ECMWF model. Figures S5 and S6 in the supporting information show that the improvement in

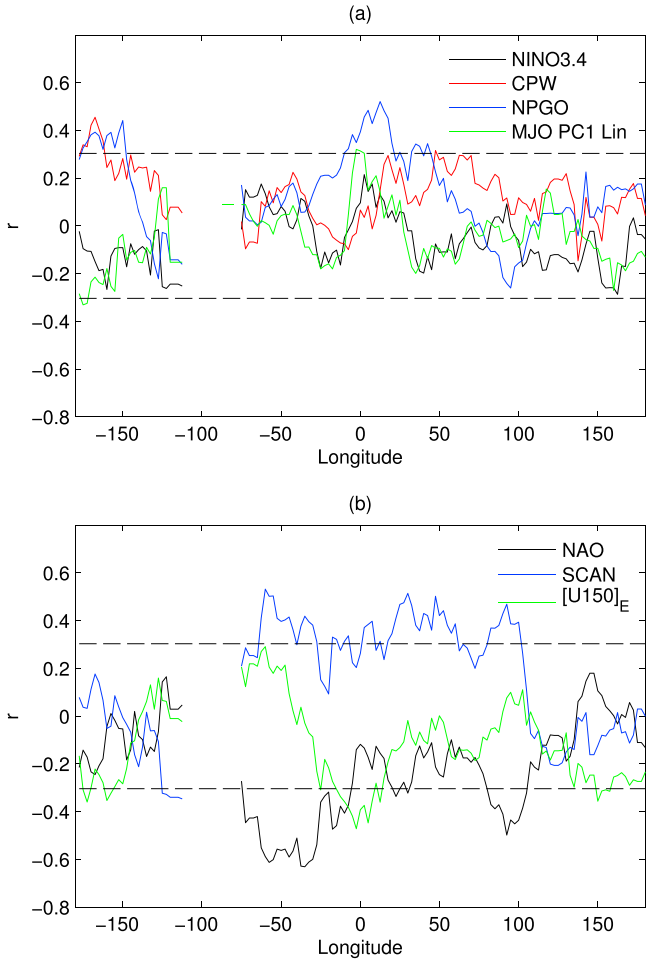

Figure 3. Correlation between seasonal mean blocking frequency at each longitude and some selected climate indices, based on observations and plotted into two panels for readability reasons. See supporting information for definitions of all indices. No values are given at longitudes where the blocking climatology is zero (see Figure 1b). The 95% significance thresholds are indicated by the black horizontal dashed lines; according to a *t* test assuming each year is independent from another.

the tropical relaxation experiments is not related to changes in the mean flow and must therefore arise from a better representation of tropical variability.

In previous studies about the NAO, we found that stratospheric variability can account for a significant part (about 25%) of the observed NAO variability on interannual and decadal timescales [*Greatbatch et al.*, 2012a, 2012b]. The bad performance of CLIM-STRAT-NH in the blocking variability as found here can partly be understood when considering the correlation between seasonal mean blocking anomalies and the NAO index (Figure 3b). The blocking anomalies are connected with the NAO index (for definitions of the NAO and following indices, though standard, see supporting information) only over the North Atlantic (about 70°W–20°W) and not over Europe, where most of the blocking variability takes place. The weak performance of CLIM-STRAT-NH in terms of blocking over the North Atlantic gives further evidence that the NAO and blocking are two distinct phenomena. Blocking anomalies over continental Europe are, however, significantly correlated with the time series of the Scandinavian pattern (consistent with *Barriopedro et al.* [2006]), a pattern that we find to be well represented in the relaxation experiments CLIM-TROPICS and OBS-TROPICS, and not in CLIM-STRAT-NH (not shown).

OBS-TROPICS shows influence from extratropical SST and sea ice on blocking, with particular success over Europe. Regression of SST on blocking anomalies averaged over Europe (20°W to 20°E; see supporting information Figure S7) reveals a significant extratropical SST signal that resembles the North Pacific Gyre Oscillation (NPGO) [*Di Lorenzo et al.*, 2010], with warm SST anomalies north of 40°N and cool anomalies around

Table 1. Lagged Composites of Anomalous European Blocking Frequency (Pentad BI Averaged Between 20°W and 20°E, Values Given in Percent) Taken From ERA-Interim Data [*Dee et al.*, 2011] With Respect to Each MJO Phase Derived for DJF Data From 1979/1980 to 2012/2013, Downloaded From http://cawcr.gov.au/ staff/mwheeler/maproom/RMM/ RMM1RMM2.74toRealtime.txt [*Wheeler and Hendon*, 2004][a]

MJO Phase	1	2	3	4	5	6	7	8	|MJO| < 0.2
Lag 0	0.80	**−2.62**	0.22	**−3.04**	**−3.23**	−0.68	**3.62**	**5.74**	0.29
Lag 1	−0.39	−0.14	−0.76	**−3.63**	**−1.45**	**2.65**	**3.50**	1.18	**6.10**
Lag 2	−0.25	**3.46**	**−2.01**	**−3.47**	0.71	**5.76**	**2.82**	0.70	**5.16**
Lag 3	1.28	0.14	**−1.81**	−0.91	**1.85**	**6.67**	0.61	**2.08**	**−2.27**

[a]Only days with an MJO amplitude greater than 1 are considered for each MJO phase, whereas the last column shows lagged blocking composites after days characterized by an MJO amplitude less than 0.2, regardless of MJO phase. Lag *n* refers to the BI averaged over the pentad centered on the 5*n*th day after the day of occurrence of the MJO of the specified phase and composite values significantly different from zero at the 95% level according to a two-sided *t* test that are in boldface.

Hawaii. This is confirmed in Figure 3a, showing significant positive correlations between blocking over Europe and the NPGO index (there are also significant positive correlations between blocking over the eastern North Pacific and the NPGO).

One candidate to explain the tropical influence on blocking over the North Pacific is El Niño Southern Oscillation (ENSO) that has been found to impact North and South Pacific blocking, e.g., leading to more intense and frequent blocking over the eastern North Pacific during La Niña events [*Renwick and Wallace*, 1996; *Renwick and Revell*, 1999; *Wiedenmann et al.*, 2002; *Barriopedro et al.*, 2006]. DJF seasonal mean blocking variability over the North Pacific is slightly anticorrelated with ENSO, using the NINO3.4 index as a proxy (see Figure 3a), although this correlation is not significant, in contrast to the previously mentioned papers that find a significant negative correlation. However, we find a significant positive correlation between blocking in the North Pacific region and both the Central Pacific Warming (CPW) and, as noted before, the NPGO indices. Variability of CPW therefore is a first possible explanation for the success of CLIM-TROPICS in the Pacific sector.

A second candidate for the improvement in blocking variability due to tropical relaxation is the intraseasonal Madden-Julian Oscillation (MJO), acting as a source for Rossby waves affecting the North Pacific and North Atlantic sectors [e.g., *Cassou*, 2008; *Lin et al.*, 2009; *Yoo et al.*, 2012]. Our Table 1 shows the connection between MJO activity and blocking anomalies over Europe (20°W to 20°E) on short timescales (0 to 3 pentads lag), for the period 1979/1980 to 2012/2013. Consistent with *Cassou* [2008] and *Vitart and Molteni* [2010], a decrease in European blocking is found after MJO phases 3 and 4 that are associated with convection over the eastern Indian ocean, and an increase in blocking after MJO phases 6 and 7 that are associated with convection over the western tropical Pacific. Interestingly, an increase in European blocking can also be found after days when the MJO amplitude is lower than 0.2 (inactive MJO). Recently, *Lin et al.* [2015] also pointed out an influence of interannual MJO variability on the winter NAO, using an index based on MJO-phase occurrence that is positive during winters with frequent phases 4 and 5 and infrequent phase 7. We only find a few longitudes, where seasonal mean blocking anomalies are significantly correlated with the MJO variability index as defined by *Lin et al.* [2015] (labeled MJO PC1 Lin in Figure 3a). *Vitart and Molteni* [2010] found that MJO propagation speed impacts the MJO influence on the extratropics, whereas *Bechtold et al.* [2008] pointed out that, in the ECMWF model, propagation speed of MJO-related convection is not realistic, although MJO *amplitude* is quite realistic. Therefore, our experiments without tropical relaxation do not have a realistic MJO *variability*, whereas MJO variability in experiments with tropical relaxation is, de facto, very close to the MJO variability in the reanalysis. This could explain part of the improved performance of CLIM-TROPICS and OBS-TROPICS at simulating blocking variability shown here. Recently, *Gollan and Greatbatch* [2015] found that equatorial anomalies in the upper tropospheric zonal mean zonal wind, which are to a large extent forced by MJO activity but are independent of ENSO, can impact the extratropics (the index being labeled $[U150]_E$). Consistently, there is a significant negative correlation between blocking over Europe and $[U150]_E$ (Figure 3b), an example being the winter of 1962/1963 [*Greatbatch et al.*, 2015]. The improved blocking climatology due to tropical relaxation can probably be explained in analogy to the discussion about interannual variability of blocking, i.e., the better representation of CPW variability and MJO variability in the tropical relaxation experiments.

On decadal timescales, the tropically forced experiment with climatological SST and sea ice (CLIM-TROPICS) has a better skill in the Pacific region compared to OBS-TROPICS that knows about the observed variability of SST and sea ice (and OBS-NO has no skill). This is consistent with *Greatbatch et al.* [2012a] (see discussions therein), who find that prescribing SST and sea ice yields a trend in geopotential height of the wrong sign over the North Pacific during the ERA-40 period, whereas it improves trends over the Atlantic-Eurasian sector, as in the present study here. Over the Atlantic-Eurasian sector, the experiment with prescribed observed SST and sea ice in addition to tropical relaxation (OBS-TROPICS) is the only experiment that has statistically significantly skill on decadal timescales. Also note that in the ensemble mean of OBS-TROPICS, the amplitude of blocking anomalies is enhanced in comparison to the other experiments, suggesting that there is some positive feedback from extratropical SST and sea ice. As discussed for interannual variability, SST anomalies associated with the NPGO have an impact on European blocking, although further research is needed to investigate possible mechanisms for this link.

Finally, it is important to note that a large part of the observed blocking variability cannot be explained by our relaxation experiments, pointing to the importance of extratropical tropospheric dynamics for explaining the variability in observed blocking frequency. In particular, the reduction in amplitude in the ensemble mean compared to single realizations by about 50% (see Figures 1c, 2, and S2) points to the fact that internal tropospheric dynamics have an important role to play for midlatitude blocking and that the tropical influence as shown by our relaxation experiments can only trigger part of the midlatitude blocking variability. Nevertheless, our results do show that variability in both the tropics and extratropical SST and sea ice have a systematic effect on blocking that is important for predictability.

Acknowledgments

We are grateful to the ECMWF for the provision of the model and the use of computer facilities to carry out the model runs reported here. During the time this work was carried out, G.G. was supported by the DFG under ISOLAA (GR 3653/4-1), a project within the Priority Programme 1158. R.J.G. is grateful to GEOMAR for the continuing support. Model data used in this paper are available from the corresponding author via e-mail. We also want to thank two anonymous reviewers for their helpful comments on the first version of the manuscript.

References

Anstey, J. A., P. Davini, L. J. Gray, T. J. Woollings, N. Butchart, C. Cagnazzo, B. Christiansen, S. C. Hardiman, S. M. Osprey, and S. Yang (2013), Multi-model analysis of Northern Hemisphere winter blocking: Model biases and the role of resolution, *J. Geophys. Res. Atmos.*, *118*, 3956–3971, doi:10.1002/jgrd.50231.

Barnes, E. A., J. Slingo, and T. Woollings (2012), A methodology for the comparison of blocking climatologies across indices, models and climate scenarios, *Clim. Dyn.*, *38*(11–12), 2467–2481, doi:10.1007/s00382-011-1243-6.

Barnes, E. A., E. Dunn-Sigouin, G. Masato, and T. Woollings (2014), Exploring recent trends in Northern Hemisphere blocking, *Geophys. Res. Lett.*, *41*, 638–644, doi:10.1002/2013GL058745.

Barriopedro, D., R. García-Herrera, A. R. Lupo, and E. Hernández (2006), A climatology of Northern Hemisphere blocking, *J. Clim.*, *19*(6), 1042–1063, doi:10.1175/JCLI3678.1.

Bechtold, P., M. Köhler, T. Jung, F. Doblas-Reyes, M. Leutbecher, M. J. Rodwell, F. Vitart, and G. Balsamo (2008), Advances in simulating atmospheric variability with the ECMWF model: From synoptic to decadal time-scales, *Q. J. R. Meteorol. Soc.*, *134*(634), 1337–1351, doi:10.1002/qj.289.

Cassou, C. (2008), Intraseasonal interaction between the Madden-Julian Oscillation and the North Atlantic Oscillation, *Nature*, *455*(7212), 523–527, doi:10.1038/nature07286.

Dee, D. P., et al. (2011), The ERA-Interim reanalysis: Configuration and performance of the data assimilation system, *Q. J. R. Meteorol. Soc.*, *137*(656), 553–597, doi:10.1002/qj.828.

Di Lorenzo, E., K. M. Cobb, J. C. Furtado, N. Schneider, B. T. Anderson, A. Bracco, M. A. Alexander, and D. J. Vimont (2010), Central Pacific El Niño and decadal climate change in the North Pacific Ocean, *Nat. Geosci.*, *3*(11), 762–765, doi:10.1038/ngeo984.

Dunn-Sigouin, E., and S. W. Son (2013), Northern Hemisphere blocking frequency and duration in the CMIP5 models, *J. Geophys. Res. Atmos.*, *118*, 1179–1188, doi:10.1002/jgrd.50143.

Flato, G., et al. (2013), Evaluation of climate models, in *Climate Change 2013: The Physical Science Basis. Contribution of Working Group I to the Fifth Assessment Report of the Intergovernmental Panel on Climate Change*, edited by V. B. Stocker et al., pp. 741–882, Cambridge Univ. Press, Cambridge, U. K., and New York, doi:10.1017/CBO9781107415324.

Francis, J. A., and S. J. Vavrus (2012), Evidence linking Arctic amplification to extreme weather in midlatitudes, *Geophys. Res. Lett.*, *39*, L06801, doi:10.1029/2012GL051000.

Gollan, G., and R. J. Greatbatch (2015), On the extratropical influence of variations of the upper-tropospheric equatorial zonal-mean zonal wind during boreal winter, *J. Clim.*, *28*(1), 168–185, doi:10.1175/JCLI-D-14-00185.1.

Greatbatch, R. J., G. Gollan, T. Jung, and T. Kunz (2012a), Factors influencing Northern Hemisphere winter mean atmospheric circulation anomalies during the period 1960/61 to 2001/02, *Q. J. R. Meteorol. Soc.*, *138*(669), 1970–1982, doi:10.1002/qj.1947.

Greatbatch, R. J., G. Gollan, and T. Jung (2012b), An analysis of trends in the boreal winter mean tropospheric circulation during the second half of the 20th century, *Geophys. Res. Lett.*, *39*, L13809, doi:10.1029/2012GL052243.

Greatbatch, R. J., G. Gollan, T. Jung, and T. Kunz (2015), Tropical origin of the severe European winter of 1962/1963, *Q. J. R. Meteorol. Soc.*, *141*(686), 153–165, doi:10.1002/qj.2346.

Hamill, T. M., and G. N. Kiladis (2014), Skill of the MJO and Northern Hemisphere blocking in GEFS medium-range reforecasts, *Mon. Weather Rev.*, *142*(2), 868–885, doi:10.1175/MWR-D-13-00199.1.

Hoerling, M. P., J. W. Hurrell, and T. Xu (2001), Tropical origins for recent North Atlantic climate change, *Science*, *292*(5514), 90–92, doi:10.1126/science.1058582.

Hoskins, B. J., M. E. McIntyre, and A. W. Robertson (1985), On the use and significance of isentropic potential vorticity maps, *Q. J. R. Meteorol. Soc.*, *111*(470), 877–946, doi:10.1002/qj.49711147002.

Hurrell, J. W., and C. Deser (2010), North Atlantic climate variability: The role of the North Atlantic Oscillation, *J. Mar. Syst.*, *79*(3–4), 231–244, doi:10.1016/j.jmarsys.2009.11.002.

Jung, T., M. J. Miller, and T. N. Palmer (2010), Diagnosing the origin of extended-range forecast errors, *Mon. Weather Rev.*, *138*(6), 2434–2446, doi:10.1175/2010MWR3255.1.

Jung, T., F. Vitart, L. Ferranti, and J.-J. Morcrette (2011), Origin and predictability of the extreme negative NAO winter of 2009/10, *Geophys. Res. Lett.*, *38*, L07701, doi:10.1029/2011GL046786.

Jung, T., et al. (2012), High-resolution global climate simulations with the ECMWF model in project Athena: Experimental design, model climate, and seasonal forecast skill, *J. Clim.*, *25*(9), 3155–3172, doi:10.1175/JCLI-D-11-00265.1.

Lin, H., G. Brunet, and J. Derome (2009), An observed connection between the North Atlantic Oscillation and the Madden-Julian Oscillation, *J. Clim.*, *22*(2), 364–380, doi:10.1175/2008JCLI2515.1.

Lin, H., G. Brunet, and B. Yu (2015), Interannual variability of the Madden-Julian Oscillation and its impact on the North Atlantic Oscillation in the boreal winter, *Geophys. Res. Lett.*, *42*, 5571–5576, doi:10.1002/2015GL064547.

Liu, J., J. A. Curry, H. Wang, M. Song, and R. M. Horton (2012), Impact of declining Arctic sea ice on winter snowfall, *Proc. Natl. Acad. Sci.*, *109*(11), 4074–4079.

Masato, G., T. Woollings, and B. J. Hoskins (2014), Structure and impact of atmospheric blocking over the Euro-Atlantic region in present-day and future simulations, *Geophys. Res. Lett.*, *41*, 1051–1058, doi:10.1002/2013GL058570.

Pelly, J. L., and B. J. Hoskins (2003), A new perspective on blocking, *J. Atmos. Sci.*, *60*(5), 743–755, doi:10.1175/1520-0469(2003)060<0743:ANPOB>2.0.CO;2.

Renwick, J. A., and M. J. Revell (1999), Blocking over the South Pacific and Rossby wave propagation, *Mon. Weather Rev.*, *127*(10), 2233–2247, doi:10.1175/1520-0493(1999)127<2233:BOTSPA>2.0.CO;2.

Renwick, J. A., and J. M. Wallace (1996), Relationships between North Pacific Wintertime Blocking, El Niño, and the PNA pattern, *Mon. Weather Rev.*, *124*(9), 2071–2076, doi:10.1175/1520-0493(1996)124<2071:RBNPWB>2.0.CO;2.

Sillmann, J., and M. Croci-Maspoli (2009), Present and future atmospheric blocking and its impact on European mean and extreme climate, *Geophys. Res. Lett.*, *36*, L10702, doi:10.1029/2009GL038259.

Trenberth, K. E., G. W. Branstator, D. Karoly, A. Kumar, N.-C. Lau, and C. Ropelewski (1998), Progress during TOGA in understanding and modeling global teleconnections associated with tropical sea surface temperatures, *J. Geophys. Res.*, *103*(C7), 14,291–14,324, doi:10.1029/97JC01444.

Trigo, R. M., I. F. Trigo, C. C. DaCamara, and T. J. Osborn (2004), Climate impact of the European winter blocking episodes from the NCEP/NCAR reanalyses, *Clim. Dyn.*, *23*(1), 17–28, doi:10.1007/s00382-004-0410-4.

Uppala, S. M., et al. (2005), The ERA-40 re-analysis, *Q. J. R. Meteorol. Soc.*, *131*(612), 2961–3012, doi:10.1256/qj.04.176.

Vitart, F., and F. Molteni (2010), Simulation of the Madden-Julian Oscillation and its teleconnections in the ECMWF forecast system, *Q. J. R. Meteorol. Soc.*, *136*(649), 842–855, doi:10.1002/qj.623.

Wallace, J. M., and D. S. Gutzler (1981), Teleconnections in the geopotential height field during the Northern Hemisphere winter, *Mon. Weather Rev.*, *109*(4), 784–812, doi:10.1175/1520-0493(1981)109<0784:TITGHF>2.0.CO;2.

Wheeler, M. C., and H. H. Hendon (2004), An all-season real-time multivariate MJO index: Development of an index for monitoring and prediction, *Mon. Weather Rev.*, *132*(8), 1917–1932, doi:10.1175/1520-0493(2004)132<1917:AARMMI>2.0.CO;2.

Wiedenmann, J. M., A. R. Lupo, I. I. Mokhov, and E. A. Tikhonova (2002), The climatology of blocking anticyclones for the Northern and Southern Hemispheres: Block intensity as a diagnostic, *J. Clim.*, *15*(23), 3459–3473, doi:10.1175/1520-0442(2002)015<3459:TCOBAF>2.0.CO;2.

Woollings, T., B. Hoskins, M. Blackburn, and P. Berrisford (2008), A new Rossby wave-breaking interpretation of the North Atlantic Oscillation, *J. Atmos. Sci.*, *65*(2), 609–626, doi:10.1175/2007JAS2347.1.

Woollings, T., A. Charlton-Perez, S. Ineson, A. G. Marshall, and G. Masato (2010), Associations between stratospheric variability and tropospheric blocking, *J. Geophys. Res.*, *115*, D06108, doi:10.1029/2009JD012742.

Wu, R., B. P. Kirtman, and K. Pegion (2006), Local air-sea relationship in observations and model simulations, *J. Clim.*, *19*(19), 4914–4932, doi:10.1175/JCLI3904.1.

Yoo, C., S. Lee, and S. B. Feldstein (2012), Mechanisms of Arctic surface air temperature change in response to the Madden-Julian Oscillation, *J. Clim.*, *25*(17), 5777–5790, doi:10.1175/JCLI-D-11-00566.1.